

# Experimental study on the thermal conductivity of a water-based ternary hybrid nanofluid incorporating MWCNTs-COOH-Fe<sub>3</sub>O<sub>4</sub>-rGO

Neşe Keklikcioğlu Çakmak<sup>1\*</sup> 

<sup>1</sup>Department of Chemical Engineering, Faculty of Engineering, Sivas Cumhuriyet University, Sivas 58140, Türkiye

**Abstract:** This study explores the thermal conductivity characteristics of ternary nanofluids composed of water-based Fe<sub>3</sub>O<sub>4</sub>-decorated carboxylated multi-walled carbon nanotubes (MWCNT-COOH), reduced graphene oxide (rGO) and Fe<sub>3</sub>O<sub>4</sub>-MWCNT-COOH/rGO ternary hybrid nanoparticles. The investigation focuses on the influence of temperature and ternary hybrid nanoparticles concentration. Ultrasonic probes were employed to ensure the stability of the nanofluid and its structural properties were analyzed using scanning electron microscopy (SEM), energy dispersive X-ray spectroscopy (EDX), X-ray powder diffraction (XRD) and Fourier-transform infrared spectroscopy (FT-IR). The transient hot-wire technique was employed to measure the thermal conductivity of all nanofluids. Thermal conductivity measurements were conducted using a KD-2 Pro thermal analyzer across a temperature range of 25-60 °C and a ternary hybrid nanoparticles volume fraction range of 0.025-0.1%. Results demonstrated that the thermal conductivity ratio increased with higher solid volume fractions and elevated temperatures. Notably, the impact of temperature became more significant at higher ternary hybrid nanoparticles concentrations. The findings also revealed a maximum thermal conductivity enhancement of approximately 50%, achieved at a ternary hybrid nanoparticles fraction of 0.1% and a temperature of 60 °C.

**Keywords:** MWCNTsCOOH- Fe<sub>3</sub>O<sub>4</sub>rGO, ultrasonification, thermal conductivity, ternary hybrid nanofluid.

## 1. Introduction

The main challenge for accelerating nanofluid studies is to enhance the performance of thermal systems such as radiators, heat exchangers, air conditioning devices and refrigerators by improving the thermophysical properties of nanofluids [1]. Choi [2] provided the emergence of the term nanofluid by using nanoparticle additives in the base fluid and in the continuation nanofluid studies, the particles and base fluids were diversified and used in many researches [3-8]. Although nanofluids are considered greatly attractive agents in heat transfer applications, it is not ensured that they have definite performance-enhancing effects [9]. In addition, nanofluids with insufficient stability cannot be applied in pumping systems due to aggregation and sedimentation complications. Problems caused by low stability lead to mechanical failure of thermal system equipment and trigger pollutants, negatively affecting heat transfer. In this concept, configurations have been created on the mono/multiple use of nanofluids and providing long-term stability and many researchers have examined and still

continue to study the positive and negative aspects of the use of designed configurations in heat transfer process [10-16]. The thermal conductivity of nanofluids used in thermal systems is great of importance [17]. The increase in thermal conductivity of nanofluids compared to conventional base fluids is due to the interaction of nanoparticles, which causes an increase in the kinetic motion of molecules at higher temperatures and therefore a higher rate of transfer of heat through the medium. The improvement of thermal conductivity varies depending on many parameters such as volume or weight fraction of the nanofluid, nanoparticle type and shape and nanofluid stability [18, 19]. To address the uncertainty in nanofluid thermal conductivity due to varying parameters, researchers have conducted several studies. For instance, Bakhtiari et al. [20] investigated the influence of temperature and volume fraction on the thermal conductivity of TiO<sub>2</sub>-Graphene/Water hybrid nanofluids, concluding that volume fraction had a more significant impact than temperature. Similarly, Taherialekouhi et al. [21] explored the thermal conductivity characteristics of water-graphene oxide/alumi-

\*Corresponding author:

Email: nkeklikcioglu@cumhuriyet.edu.tr

Cite this article as:

Çakmak-Keklikcioğlu, N. (2025). Experimental study on the thermal conductivity of a water-based ternary hybrid nanofluid incorporating MWCNTs-COOH-Fe<sub>3</sub>O<sub>4</sub>-rGO. *European Mechanical Science*, 9(1): 16-24. <https://doi.org/10.26701/ems.1591623>

History dates:

Received: 26.11.2024, Revision Request: 08.01.2025, Last Revision Received: 22.01.2025, Accepted: 02.03.2025



© Author(s) 2025. This work is distributed under <https://creativecommons.org/licenses/by/4.0/>



num oxide nanoparticles as a potential cooling fluid. In this study, where the temperature and nanofluid volume fraction ranges were indicated as 25-50 °C and 0.1-1%, respectively, it was reported that the parameter of temperature was more triggering in promoting the thermal conductivity. The highest thermal conductivity enhancement of 33.9% was ensured at the configuration of the volume fraction of 1% and temperature of 50 °C. Akghar et al. [22] carried out an experimental investigation to evaluate the changes in thermal conductivity of water ethylene glycol/TiO<sub>2</sub>-MWCNT nanofluid under varying temperatures and volume fractions. The results revealed that the volume fraction was increasingly dominant to improve thermal conductivity of hybrid nanofluid relative to temperature. A study by Kazemi et al. [23] investigated the variation of thermal conductivity using mono and hybrid Graphene/SiO<sub>2</sub> nanofluids at variety of volume fractions of 0.051% and temperature range between 25-50 °C. The study resulted with an improvement of 36.12% in thermal conductivity using Graphene-SiO<sub>2</sub>/Water hybrid nanofluid. Due to high aspect ratio, superior thermal properties and synergistic relationships of nanoparticles with each other, the idea of producing hybrid nanofluids is triggered and initiated to achieve enhancement in heat transfer and pressure drop properties. In the last 3 years, a new research direction has emerged towards combining different nanoparticles to obtain nanofluids with optimum characteristics: this is the synthesis of three-particle or ternary nanofluids (THyNFs) [24]. Ternary hybrid nanofluids (THyNF) have garnered a lot of interest nowadays because of their exceptional capacity to enhance heat transfer efficiency in comparison to conventional fluids. These innovative nanofluids exhibit significantly higher convective heat transfer coefficients and thermal conductivity, which significantly increases total heat transfer efficiency in a variety of applications [24]. A base fluid is mixed with an exclusive combination of three different kinds of nanoparticles to create these ternary hybrid nanofluids. In order to improve fluid properties, especially thermal and transport ones, ternary hybrid nanofluids combine metallic, oxide, or carbon-based nanoparticles. As a basic fluid transport property, thermal conductivity aids in the comprehension of heat transfer mechanisms and the improvement of thermal management systems. Thermal conductivity affects the power cycle's efficiency and system dependability. Furthermore, accurate fluid thermal conductivity is necessary for the design and development of innovative technologies, including energy storage devices and cooling systems [18,19]. Fluid thermal conductivity has been measured using a variety of techniques. Widely applied and appropriate for fluids, the transient hot-wire (THW) approach has very low uncertainty [20, 21]. The benefits of THW approaches include lowering convective error during experimental data processing and avoiding the end effect by using two wires. Transient hot-wire (THW) approach, which has proven to be reliable, was used in this study.

In this study, an experimental study was conducted

on Fe<sub>3</sub>O<sub>4</sub>-decorated carboxylated multi-walled carbon nanotubes (MWCNT-COOH)/reduced graphene oxide (Fe<sub>3</sub>O<sub>4</sub>-MWCNT-COOH/rGO)/water ternary nanofluids to analyze the impact of temperature and ternary hybrid nanoparticles concentration on thermal conductivity.

## 2. Experimental Section

### 2.1. Materials

The chemicals utilized in this study included ferrous chloride tetrahydrate (FeCl<sub>2</sub>·4H<sub>2</sub>O), sodium hydroxide (NaOH), nitric acid (HNO<sub>3</sub>, 70%), sulfuric acid (H<sub>2</sub>SO<sub>4</sub>, 96%) and ferric chloride hexahydrate (FeCl<sub>3</sub>·6H<sub>2</sub>O). All reagents were sourced from Sigma-Aldrich (Burlington, USA) and were used as received without further purification. Multi-walled carbon nanotubes (MWCNTs), with a purity of approximately 96%, an external diameter of 8–18 nm and lengths ranging from 10–30 μm, were synthesized using catalytic chemical vapor deposition. These were procured in their original form from Nanografi (Turkey).

### 2.2. Oxidation of MWCNTs

The oxidation of MWCNTs followed a previously established method [25]. A mixture containing 400 mg of MWCNTs and 100 mL of concentrated HNO<sub>3</sub> and H<sub>2</sub>SO<sub>4</sub> (in a 1:3 ratio; 25 mL HNO<sub>3</sub> and 75 mL H<sub>2</sub>SO<sub>4</sub>) was subjected to ultrasonication for 140 minutes. This mixture was then transferred to a flask with a condenser and refluxed under vigorous agitation at 75 °C for six hours. Upon cooling to room temperature, the suspension was centrifuged at 18,000 rpm and the solid residue was washed multiple times with deionized water until the pH of the filtrate approached neutrality. The resulting solid was dried in a vacuum oven at 80 °C for two hours and designated as MWCNT-COOH.

The cutting of MWCNTs served two purposes: (i) to introduce functional –COOH groups and (ii) to enhance the solubility of the MWCNTs in various solvents.

### 2.3. Synthesis of MWCNT-COOH-Fe<sub>3</sub>O<sub>4</sub> Hybrid Nanoparticles

The MWCNT-COOH-Fe<sub>3</sub>O<sub>4</sub> hybrid nanoparticles were synthesized via in-situ growth and chemical coprecipitation methods [26, 27]. A solution of 0.35 g MWCNT-COOH in 100 mL of water was stirred for one hour, followed by the addition of FeCl<sub>3</sub> and FeCl<sub>2</sub> salts in a 2:1 molar ratio under continuous stirring. The reaction was performed under a nitrogen atmosphere. Once the iron salts dissolved, turning the solution light orange, water-diluted NaOH was gradually introduced. Within 10 minutes, black precipitates formed, indicating the completion of the reaction. The Fe<sub>3</sub>O<sub>4</sub> nanoparticles attached are to the MWCNTs via the –COOH functional groups, which are thin enough to retain the fluid's heat

transfer characteristics when dispersed in water. The precipitates were repeatedly washed with water to eliminate chloride, sodium and hydrogen impurities before being dried at 80 °C for 24 hours. Pure Fe<sub>3</sub>O<sub>4</sub> nanoparticles were also synthesized for comparison purposes using the same procedure, but without the addition of MWCNTs to the distilled water.

#### 2.4. Synthesis of MWCNT-COOH-Fe<sub>3</sub>O<sub>4</sub>-rGO Ternary Hybrid Nanoparticles

The rGO was synthesized from natural graphite powder using a modified Hummers method, later employed to prepare the ternary hybrid nanoparticles [28–34]. Graphite oxide was dispersed in deionized (DI) water and exfoliation into individual sheets was achieved via ultrasonication at room temperature for 1 hour. To remove any unexfoliated graphite oxide, the suspension was centrifuged at 18,000 rpm for 30 minutes. The reduction and purification of rGO involved sonicating a mixture of 0.5 g graphite oxide (GO) and 5 g L-ascorbic acid in 500 mL of deoxygenated water for 30 minutes, followed by stirring at 60 °C for 36 hours. The resulting material was washed, filtered, dried and stored at room temperature. To form the hybrid material, carboxylated MWCNT-Fe<sub>3</sub>O<sub>4</sub> was introduced into the rGO suspension. The mixture was vigorously stirred and ultrasonicated for 2 hours at room temperature to promote grafting and ensure the intercalation of MWCNT-COOH-Fe<sub>3</sub>O<sub>4</sub> within the rGO nanosheets. The resulting MWCNT-COOH-Fe<sub>3</sub>O<sub>4</sub>-rGO composite was centrifuged at 18,000 rpm, thoroughly washed with DI water and dried at 80 °C for further characterization and experimentation.

#### 2.5. Characterization

The synthesized ternary hybrid nanoparticles were structurally analyzed using X-ray diffraction (XRD) (Rigaku DMAX IIIC). Morphological features were assessed with a scanning electron microscope (SEM: TESCAN MIRA3 XMU) equipped with an energy-dispersive X-ray spectrometer (EDX). Functional groups were analyzed using Fourier-transform infrared spectroscopy (FTIR: Bruker Tensor II) within the range of 4000–500 cm<sup>-1</sup>. Specimens were pressed into potassium bromide pellets for FTIR analysis.

#### 2.6. Ultrasound application

The ternary hybrid nanoparticles were dispersed in water at concentrations ranging from 0.025% to 0.1% by volume and temperatures between 25 and 60 °C. Uniform dispersion and stability of the nanofluids were achieved using a 750-W ultrasonic liquid processor (Sonics & Materials Inc., USA, VCX750 sonicator). The nanofluids were under continuous and pulsed ultrasound treatment at 20 kHz for 60 minutes in an ultrasonic device. To prevent overheating, a water bath was placed on the walls of the beaker holding the nanofluid.

The ultrasonic probe was positioned inside an acoustic foam sound-reduction enclosure. A cylindrical-diameter, cylindrical-shaped 13 mm tTi6Al4V titanium alloy probe was employed. In the continuous and pulsed processes, the probe was positioned 100 mm above the surface of the nanofluids, 10 mm below, with a frequency of 20 kHz and an amplitude level of 40%. Discrete nanoparticles or lower particle sizes were successfully produced by ultrasonication.

#### 2.7. Thermal conductivity measurement

Nanofluids with varying MWCNT-COOH-Fe<sub>3</sub>O<sub>4</sub>-rGO ratios were prepared to evaluate their thermal conductivity. A KD2 Pro thermal properties analyzer (Decagon Devices, Inc., Pullman, WA, USA) employing the transient hot-wire technique was used for measurements. Synthesis of ternary hybrid nanoparticles and the thermal conductivity setup are illustrated in ►**Figure 1**. Thermal conductivity measurements were conducted at 25, 35, 45, 55 and 60 °C. Sensor accuracy was validated through repeated calibration with water. Measurements were performed 5 minutes after immersion in a water bath to stabilize temperature. Each test involved 20 readings taken at 15-minute intervals, with the average recorded. Thermal conductivity of the base fluid (water) was measured at the start and end of each experiment, aligning with reported literature values (Table 1, [42]) for verification.

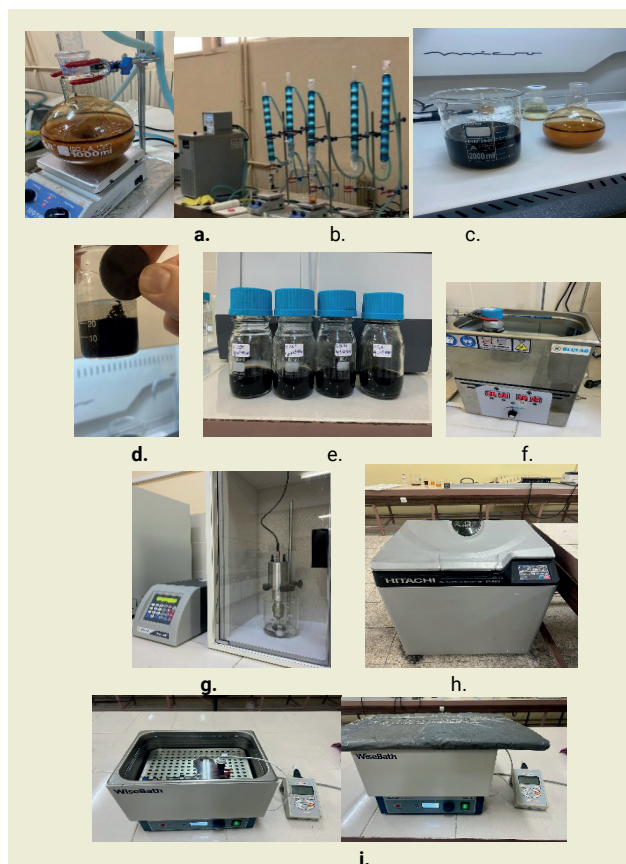


**Figure 1.** Figures of MWCNT-COOH-Fe<sub>3</sub>O<sub>4</sub>-rGO-water ternary hybrid nanofluid preparation process (a–e) f. bath sonicator g. probe sonicator h. high speed centrifuge i. thermal conductivity device and water bath.

**Table 1.** Experimental thermal conductivity ( $k$ ) of base fluid water as a function of temperature ( $T$ )

T/K	$k/(W\ m^{-1}\ K^{-1})$	
	Measured data	Reference data
298	0.611±0.002	0.6076 [42]
308	0.626±0.002	0.6240 [42]
318	0.638±0.003	0.6380 [42]
328	0.644±0.002	0.6497 [42]
333	0.650±0.004	0.6480 [42]

The “thermal conductivity ratio” is defined as follows to provide a clear investigation:

$$\text{thermal conductivity ratio} = \frac{k_{nf}}{k_{bf}}$$

### 3. Results and discussion

#### 3.1. SEM Analysis

The particle size and surface morphology of the synthesized samples and hybrid material were analyzed using SEM, as shown in ►Figure 2. The SEM images reveal that carbon nanotubes grew on both sides of the rGO sheets, which exhibit ultrathin, wrinkled, wavy and fibrous structures. The MWCNT-COOH samples appear cylindrical, with curved and entangled morphologies. Furthermore, the  $Fe_3O_4$  nanoparticles are nearly uniform in size and the SEM clearly shows their attachment to the surfaces of MWCNT-COOH.

#### 3.2. SEM-EDX Analysis

SEM-EDX analysis was performed to determine the elemental composition of the samples. This technique provides precise identification and quantification of elements in small sample volumes. The EDX spectra of GO (►Figure 3a), MWCNT-COOH (►Figure 3b), MWCNT-COOH- $Fe_3O_4$  (Fig. 3c) and MWCNT-COOH- $Fe_3O_4$ -rGO (Fig. 3d) confirm the successful deposition

of  $Fe_3O_4$  on MWCNT-COOH. The carbon (C) signal originates from the MWCNTs, while the oxygen (O) signal is attributed to functionalization with -COOH groups. The Fe signal confirms the presence of  $Fe_3O_4$ . In the ternary hybrid nanoparticles, the composition by mass is C 46%, O 29.7% and Fe 24.3%, indicating a predominant presence of these elements.

#### 3.3. XRD Analysis

The XRD patterns for GO, MWCNT-COOH and MWCNT-COOH- $Fe_3O_4$ -rGO are depicted in ►Figure 4. MWCNT-COOH exhibits peaks at  $2\theta$  values of  $25.9^\circ$  (002),  $43.0^\circ$  (100), and  $44.0^\circ$  (101) [36–38]. GO is characterized by a diffraction peak at  $2\theta = 11.2^\circ$  [39], which disappears after reduction, with rGO showing a peak at  $26.1^\circ$  [40]. The overlap of MWCNT and rGO peaks at  $26.1^\circ$  increases intensity in this region.  $Fe_3O_4$  diffraction peaks were observed at  $2\theta$  values of  $18.5^\circ$ ,  $30.3^\circ$ ,  $35.7^\circ$ ,  $43.5^\circ$ ,  $53.4^\circ$ ,  $57.2^\circ$ , and  $63.1^\circ$ , corresponding to planes (111), (220), (311), (400), (422), (511) and (440), respectively, consistent with the cubic structure and JCPDS no. 65-3107 [41]. These results confirm that GO was fully reduced to rGO and  $Fe_3O_4$  nanoparticles were successfully incorporated.

#### 3.4. FTIR Analysis

Fourier-transform infrared spectroscopy (FTIR) (►Figure 5) was employed to examine functional groups in MWCNT-COOH- $Fe_3O_4$ -rGO. Peaks at  $1550\ cm^{-1}$  and  $1346\ cm^{-1}$  correspond to C=O and C=C groups, respectively, characteristic of carbon nanotube sidewalls. The broad peak at  $3400\ cm^{-1}$  is attributed to O–H stretching in carboxylic acid groups, while the peak at  $1044\ cm^{-1}$  is associated with C–O vibrations. A peak at  $2800\ cm^{-1}$  indicates –CH stretching and the Fe–O vibration is observed at  $561\ cm^{-1}$ , confirming the presence of  $Fe_3O_4$ . These findings demonstrate effective modification of nanotubes with –COOH groups and successful integration of  $Fe_3O_4$  and rGO.

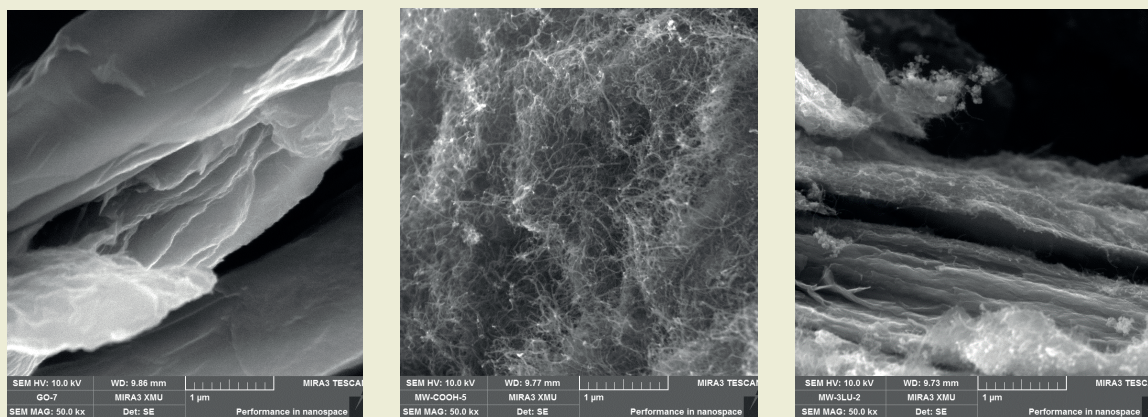


**Figure 2.** SEM images showing morphologies of GO, MWCNT-COOH and MWCNT-COOH- $Fe_3O_4$ -rGO.

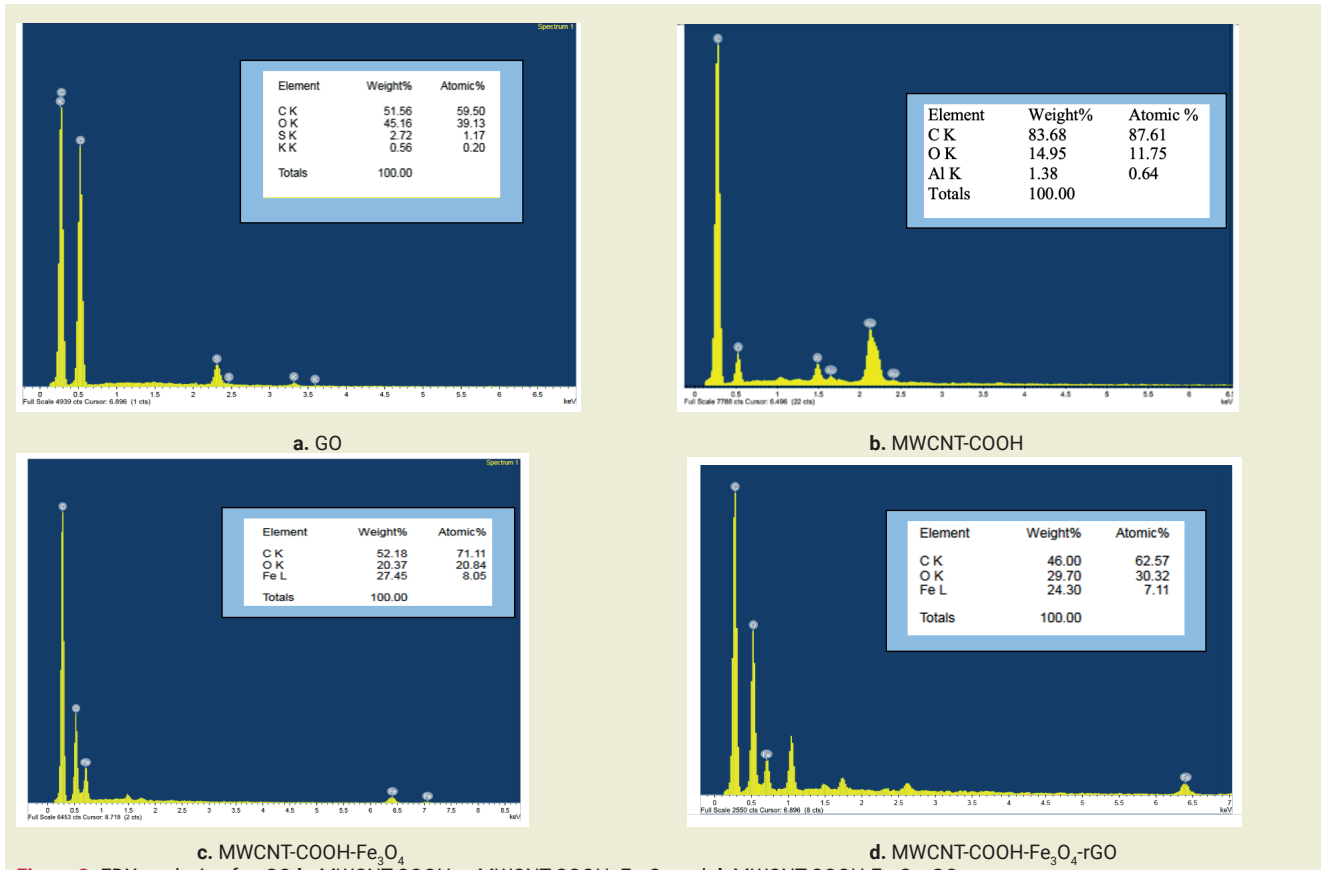


Figure 3. EDX analysis of a. GO b. MWCNT-COOH c. MWCNT-COOH-Fe<sub>3</sub>O<sub>4</sub> and d. MWCNT-COOH-Fe<sub>3</sub>O<sub>4</sub>-rGO

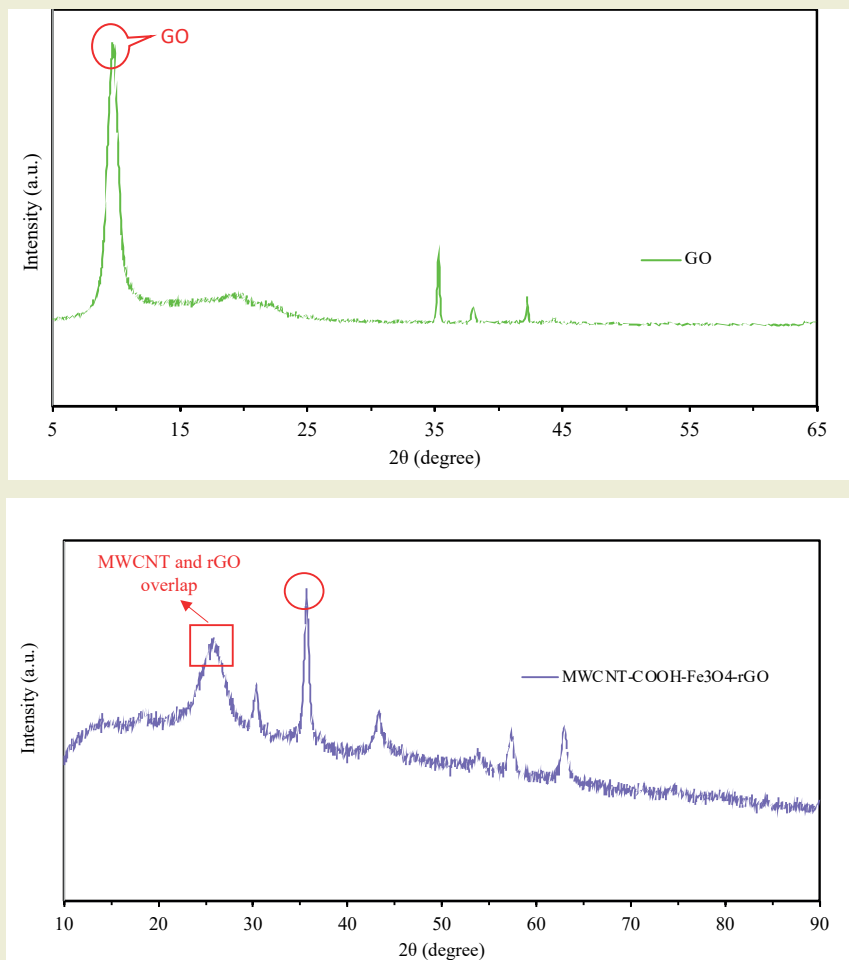


Figure 4. XRD patterns of GO, MWCNT-COOH and MWCNT-COOH-Fe<sub>3</sub>O<sub>4</sub>-rGO.

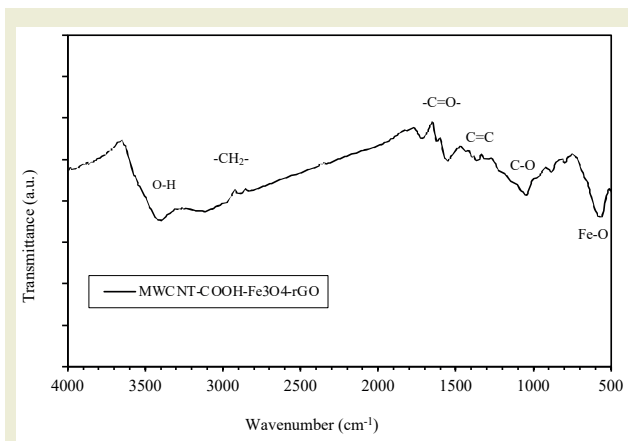


Figure 5. The FTIR spectra of MWCNT-COOH-Fe<sub>3</sub>O<sub>4</sub>-rGO

### 3.5. Thermal Conductivity Analysis

The experimental thermal conductivity of MWCNT-COOH-Fe<sub>3</sub>O<sub>4</sub>-rGO/water nanofluids was measured at temperatures ranging from 25 to 60 °C, with solid volume fractions of 0.025%, 0.05%, 0.075% and 0.1%, as shown in ►Figures 6 and 7. Thermal conductivity is influenced by nanoparticle concentration, temperature, and the thermal properties of both the base fluid and hybrid nanoparticles.

The data presented in ►Figures 6 and 7 illustrate a non-linear increase in thermal conductivity with temperature for all the studied nanofluids. At lower temperatures (25–30 °C), thermal conductivity values are modest, but a significant increase is observed at temperatures exceeding 30 °C, with notable enhancements compared to the base fluid. This behavior is attributed primarily to the intensified Brownian motion of nanoparticles at elevated temperatures, which outweighs the reduced thermal conductivity caused by thinner liquid layers surrounding the particles. Although Brownian motion is the primary driver of thermal conductivity variation, other factors, such as the high aspect ratio of the particles, nanoparticle agglomeration and the increased surface area of suspended nanostructures, also contribute to this trend. The concentration of the nanohybrid also plays a crucial role. Higher concentrations result in greater thermal conductivity due to the intrinsic high thermal transfer properties of nanoparticles. For instance, the highest thermal conductivity recorded was 0.988 W/mK at 60 °C for a 0.1% concentration of MWCNT-COOH-Fe<sub>3</sub>O<sub>4</sub>-rGO in water. Thermal conductivity generally exhibits a non-linear increase with rising nanohybrid concentrations, where low concentrations lead to slow increases due to thermal contact resistance. Additionally, overlapping or interacting liquid layers surrounding the nanoparticles can further enhance thermal conductivity.

Heat conduction is a microscopic phenomenon that is impossible to see or fully describe through experimentation. The ordered organization of liquid molecules on the surface of nanoparticles has been identified by sev-

eral studies as one of the main mechanisms displayed in relation to the abnormally high thermal conductivity of nanofluids. The interfacial layer, which was initially described and described by Choi et al. [2], is the term used to describe this organized layer structure that forms a shell at the surfaces of nanoparticles. It has been demonstrated that heat transfer from nanoparticles to the base liquid is interestingly influenced by the thickness of the interfacial layer. However, because of its incredibly small size, the interface layer remains exceedingly challenging to characterize experimentally. Some studies attempted to address this by examining and assessing the impact of the interfacial layer on the anomalous thermal conductivity using numerous simulations. The matter has been addressed in recent years by a number of simulated and experimental investigations that look at and assess how the interface layer affects thermal conductivity.

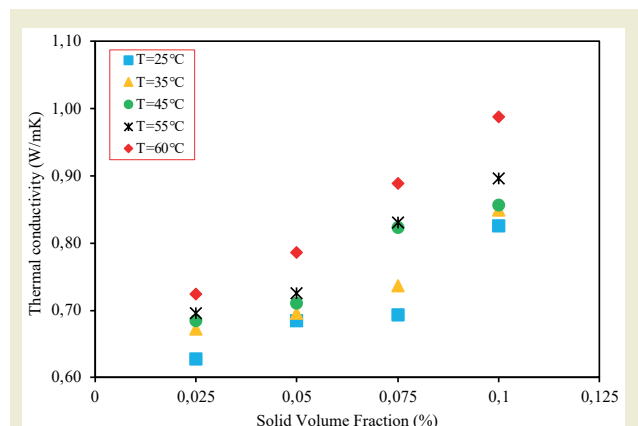


Figure 6. The ternary hybrid nanofluids' thermal conductivity in relation to the solid volume fraction at various temperatures.

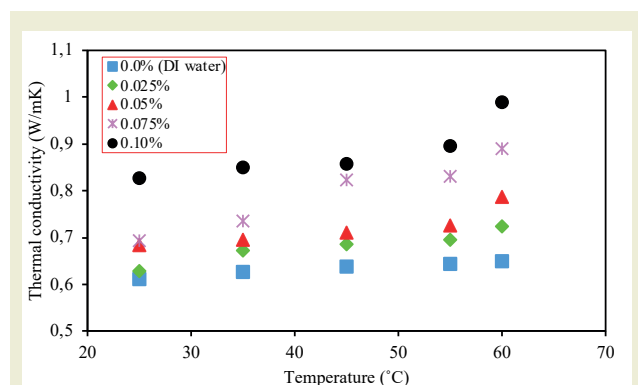
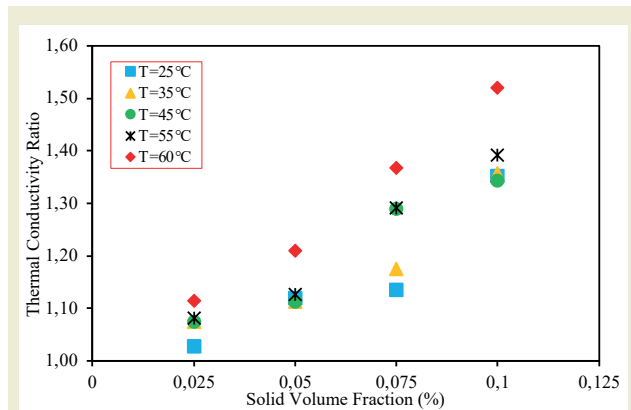


Figure 7. The ternary hybrid nanofluids' thermal conductivity in relation to temperature for different nanofluid samples.

### 3.6. Thermal Conductivity Ratio Analysis

Figures 8 and 9 provide a detailed depiction of the thermal conductivity ratio as a function of temperature and solid volume fraction. The variation in the thermal conductivity ratio with solid volume fraction becomes significantly more pronounced at higher temperatures than at lower ones. This can be attributed to the greater impact of temperature on the mobility of particles at higher concentrations. The data also demonstrate that

the influence of temperature on the thermal conductivity ratio becomes increasingly significant with larger solid volume fractions, where particle motion is more sensitive to temperature changes. A maximum thermal conductivity enhancement of approximately 50% was recorded at 60 °C with a solid volume fraction of 0.1%. These findings underscore the potential of hybrid nanofluids to significantly improve the heat transfer performance of base fluids under optimized conditions.



**Figure 8.** Change in the ternary hybrid nanofluid's thermal conductivity ratio with solid volume fraction

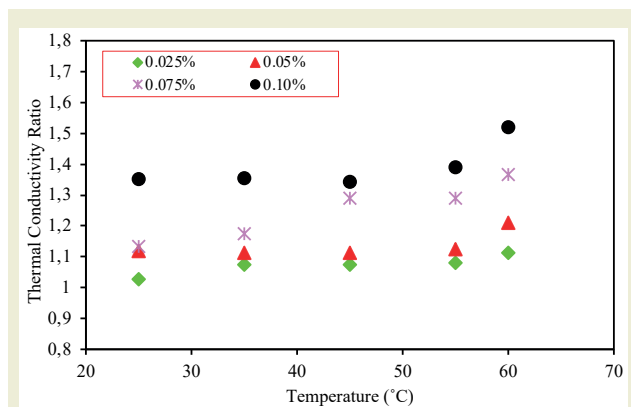


**Figure 9.** Change in the ternary hybrid nanofluid's thermal conductivity ratio with temperature.

## 4. Conclusion

This study investigated the thermal conductivity of MWCNT-COOH-Fe<sub>3</sub>O<sub>4</sub>-rGO hybrid nanofluids across temperatures ranging from 25 °C to 60 °C, with solid volume fractions of 0.025%, 0.05%, 0.075% and 0.1%. The experimental results demonstrated that both temperature and solid volume fraction significantly influence thermal conductivity. Specifically, thermal conductivity increased consistently with rising temperatures and solid volume fractions. Moreover, the findings revealed that at elevated temperatures, the influence of solid volume fraction on the thermal conductivity ratio was more pronounced compared to lower temperatures. Similarly, higher solid volume fractions

amplified the effect of temperature on the thermal conductivity ratio, emphasizing the synergistic relationship between these parameters. The study concluded that the maximum observed enhancement in thermal conductivity was approximately 50%, achieved at a temperature of 60 °C and a solid volume fraction of 0.1%. These findings demonstrate how hybrid nanofluids may improve heat transfer efficiency in particular circumstances. Nanofluids have proven to be highly suitable for a variety of heat transfer applications, including electronic cooling, refrigeration systems, heat exchangers, and solar thermal systems [43-46]. However, more research is required to determine whether nanofluids are appropriate for life cycle analysis of these physical systems. It is necessary to conduct thorough research on the economic implications of nanofluid. Long-term, very stable nanofluids, on the other hand, have superior thermophysical characteristics that enhance system performance and allow for several operating cycles, hence proving to be economically advantageous. The investigation indicates that, in comparison to the basic fluids (deionized water), hybrid nanofluids based on ternary hybrid nanoparticles have superior thermal properties. Consequently, these hybrid nanofluids are the nanofluids of the future for electronic cooling or heat exchange systems.

## Research ethics

Not applicable.

## Author contributions

The author solely conducted all stages of this research.

## Competing interests

The author state no conflict of interest.

## Research funding

None declared.

## Data availability

The raw data can be obtained on request from the author.

## Peer-review

Externally peer-reviewed.

## Orcid

Neşe Keklikcioğlu Çakmak  <https://orcid.org/0000-0002-8634-9232>

## References

- [1] Sarkar, J., Ghosh, P., & Adil, A. (2015). A review on hybrid nanofluids: recent research, development and applications. *Renewable and Sustainable Energy Reviews*, 43, 164-177.
- [2] Choi, S. U., & Eastman, J. A. (1995). Enhancing thermal conductivity of fluids with nanoparticles (No. ANL/MSD/CP-84938; CONF-951135-29). Argonne National Lab.(ANL), Argonne, IL (United States).
- [3] Gupta, M., Singh, V., & Said, Z. (2020). Heat transfer analysis using zinc Ferrite/water (Hybrid) nanofluids in a circular tube: An experimental investigation and development of new correlations for thermophysical and heat transfer properties. *Sustainable Energy Technologies and Assessments*, 39, 100720.
- [4] Sundar, L. S., Sintie, Y. T., Said, Z., Singh, M. K., Punnaiah, V., & Sousa, A. C. (2020). Energy, efficiency, economic impact, and heat transfer aspects of solar flat plate collector with Al<sub>2</sub>O<sub>3</sub> nanofluids and wire coil with core rod inserts. *Sustainable Energy Technologies and Assessments*, 40, 100772.
- [5] Çakmak, N. K. (2019). Experimental Study of Thermal Conductivity of Boric Acid– Water Solutions. *Heat Transfer Research*, 50(17).
- [6] Keklikcioğlu, O., Dagdevir, T., & Özceylan, V. (2019). Heat transfer and pressure drop investigation of graphene nanoplatelet-water and titanium dioxide-water nanofluids in a horizontal tube. *Applied Thermal Engineering*, 162, 114256.
- [7] Yarmand, H., Gharekhani, S., Shirazi, S. F. S., Amiri, A., Alehashem, M. S., Dahari, M., & Kazi, S. N. (2016). Experimental investigation of thermo-physical properties, convective heat transfer and pressure drop of functionalized graphene nanoplatelets aqueous nanofluid in a square heated pipe. *Energy Conversion and Management*, 114, 38-49.
- [8] Akdag, U., Akcay, S., & Demiral, D. (2014). Heat transfer enhancement with laminar pulsating nanofluid flow in a wavy channel. *International Communications in Heat and Mass Transfer*, 59, 17-23.
- [9] Sahoo, R. R. (2020). Thermo-hydraulic characteristics of radiator with various shape nanoparticle-based ternary hybrid nanofluid. *Powder technology*, 370, 19-28.
- [10] Urmi, W., Rahman, M. M., & Hamzah, W. A. W. (2020). An experimental investigation on the thermophysical properties of 40% ethylene glycol based TiO<sub>2</sub>-Al<sub>2</sub>O<sub>3</sub> hybrid nanofluids. *International Communications in Heat and Mass Transfer*, 116, 104663.
- [11] Akhavan-Behabadi, M. A., Shahidi, M., & Aligoodarz, M. R. (2015). An experimental study on heat transfer and pressure drop of MWCNT–water nano-fluid inside horizontal coiled wire inserted tube. *International Communications in Heat and Mass Transfer*, 63, 62-72.
- [12] Wusiman, K., Jeong, H., Tulugan, K., Afrianto, H., & Chung, H. (2013). Thermal performance of multi-walled carbon nanotubes (MWCNTs) in aqueous suspensions with surfactants SDBS and SDS. *International Communications in Heat and Mass Transfer*, 41, 28-33.
- [13] Sundar, L. S., Bhramara, P., Kumar, N. R., Singh, M. K., & Sousa, A. C. (2017). Experimental heat transfer, friction factor and effectiveness analysis of Fe<sub>3</sub>O<sub>4</sub> nanofluid flow in a horizontal plain tube with return bend and wire coil inserts. *International Journal of Heat and Mass Transfer*, 109, 440-453.
- [14] Ghozatloo, A., Shariaty-Niasar, M., & Rashidi, A. M. (2013). Preparation of nanofluids from functionalized Graphene by new alkaline method and study on the thermal conductivity and stability. *International Communications in Heat and Mass Transfer*, 42, 89-94.
- [15] Chakraborty, S., & Panigrahi, P. K. (2020). Stability of nanofluid: A review. *Applied Thermal Engineering*, 174, 115259.
- [16] Das, P. K., Mallik, A. K., Ganguly, R., & Santra, A. K. (2016). Synthesis and characterization of TiO<sub>2</sub>–water nanofluids with different surfactants. *International Communications in Heat and Mass Transfer*, 75, 341-348.
- [17] Esfe, M. H., & Hajmohammad, M. H. (2017). Thermal conductivity and viscosity optimization of nanodiamond-Co<sub>3</sub>O<sub>4</sub>/EG (40: 60) aqueous nanofluid using NSGA-II coupled with RSM. *Journal of Molecular Liquids*, 238, 545-552.
- [18] Sundar, L. S., Singh, M. K., & Sousa, A. C. (2013). Thermal conductivity of ethylene glycol and water mixture based Fe<sub>3</sub>O<sub>4</sub> nanofluid. *International communications in heat and mass transfer*, 49, 17-24.
- [19] Javadi, F. S., Sadeghipour, S., Saidur, R., BoroumandJazi, G., Rahmati, B., Elias, M. M., & Soheli, M. R. (2013). The effects of nanofluid on thermophysical properties and heat transfer characteristics of a plate heat exchanger. *International Communications in Heat and Mass Transfer*, 44, 58-63.
- [20] Bakhtiari, R., Kamkari, B., Afrand, M., & Abdollahi, A. (2021). Preparation of stable TiO<sub>2</sub>-Graphene/Water hybrid nanofluids and development of a new correlation for thermal conductivity. *Powder Technology*, 385, 466-477.
- [21] Taherialekouhi, R., Rasouli, S., & Khosravi, A. (2019). An experimental study on stability and thermal conductivity of water-graphene oxide/aluminum oxide nanoparticles as a cooling hybrid nanofluid. *International Journal of Heat and Mass Transfer*, 145, 118751.
- [22] Akhgar, A., & Toghraie, D. (2018). An experimental study on the stability and thermal conductivity of water-ethylene glycol/TiO<sub>2</sub>-MWCNTs hybrid nanofluid: developing a new correlation. *Powder Technology*, 338, 806-818.
- [23] Kazemi, I., Sefid, M., & Afrand, M. (2020). Improving the thermal conductivity of water by adding mono & hybrid nano-additives containing graphene and silica: A comparative experimental study. *International Communications in Heat and Mass Transfer*, 116, 104648.
- [24] Adun, H., Kavaz, D., & Dagbasi, M. (2021). Review of ternary hybrid nanofluid: Synthesis, stability, thermophysical properties, heat transfer applications, and environmental effects. *Journal of Cleaner Production*, 328, 129525.
- [25] Park, H. J., Kim, J., Chang, J. Y., & Theato, P. (2008). Preparation of transparent conductive multilayered films using active pentafluorophenyl ester modified multiwalled carbon nanotubes. *Langmuir*, 24(18), 10467-10473.
- [26] Şentürk, İ., & Keklikcioğlu Çakmak, N., (2025). Use of magnetic nanoparticle loaded functionalized multiwalled carbon nanotubes for effective removal of Maxilon red GRL from aqueous solutions. *Journal Of The Iranian Chemical Society*, vol.22, no.1, 141-159.
- [27] Hummers Jr, W. S., & Offeman, R. E. (1958). Preparation of graphitic oxide. *Journal of the american chemical society*, 80(6), 1339-1339.
- [28] Saleh, B., & Sundar, L. S. (2021). Thermal efficiency, heat transfer, and friction factor analyses of MWCNT+ Fe<sub>3</sub>O<sub>4</sub>/water hybrid nanofluids in a solar flat plate collector under thermosyphon condition. *Processes*, 9(1), 180.
- [29] Marcano, D. C., Kosynkin, D. V., Berlin, J. M., Sinitiskii, A., Sun, Z., Slesarev, A., ... & Tour, J. M. (2010). Improved synthesis of graphene oxide. *ACS nano*, 4(8), 4806-4814.
- [30] Xiang, Q., Yu, J., & Jaroniec, M. (2011). Enhanced photocatalytic H<sub>2</sub>-production activity of graphene-modified titania nanosheets. *Nanoscale*, 3(9), 3670-3678.
- [31] Said, Z., Çakmak, N. K., Sharma, P., Sundar, L. S., Inayat, A., Keklikcioğlu, O., & Li, C. (2022). Synthesis, stability, density, viscosity of ethylene glycol-based ternary hybrid nanofluids: Experimental investigations and model-prediction using modern machine learning techniques. *Powder Technology*, 400, 117190.
- [32] Keklikcioğlu Çakmak, N. (2020). The impact of surfactants on the stability and thermal conductivity of graphene oxide de-ionized water nanofluids. *Journal of Thermal Analysis and Calorimetry*, 139(3), 1895-1902.
- [33] Basu, A. K., Sah, A. N., Pradhan, A., & Bhattacharya, S. (2019). Poly-L-Lysine functionalised MWCNT-rGO nanosheets based 3-d hybrid structure for femtomolar level cholesterol detection using cantilever based sensing platform. *Scientific reports*, 9(1), 3686.
- [34] Han, C. L., Zou, A. L., Wang, G. D., Liu, Y., Li, N., Zhang, H. X., ... & Blackie, E. (2022). Study on 3D multi-performance composite films of Fe<sub>3</sub>O<sub>4</sub> decorated CNTs/graphene oxide. *Diamond and Related Materials*, 124, 108953.
- [35] Zhou, J., Pan, K., Qu, G., Ji, W., Ning, P., Tang, H., & Xie, R. (2022).

- rGO/MWCNTs-COOH 3D hybrid network as a high-performance electrochemical sensing platform of screen-printed carbon electrodes with an ultra-wide detection range of Cd (II) and Pb (II). *Chemical Engineering Journal*, 449, 137853.
- [36] Das, R., Bee Abd Hamid, S., Eaqub Ali, M., Ramakrishna, S., & Yongzhi, W. (2015). Carbon nanotubes characterization by X-ray powder diffraction—a review. *Current Nanoscience*, 11(1), 23-35.
- [37] Salam, M. A., & Burk, R. (2017). Synthesis and characterization of multi-walled carbon nanotubes modified with octadecylamine and polyethylene glycol. *Arabian Journal of Chemistry*, 10, S921-S927.
- [38] Al-Jammal, N., Abdullah, T. A., Juzsakova, T., Zsirka, B., Cretescu, I., Vágvölgyi, V., ... & Domokos, E. (2020). Functionalized carbon nanotubes for hydrocarbon removal from water. *Journal of Environmental Chemical Engineering*, 8(2), 103570.
- [39] Zou, H., Li, X., Zhang, Y., Wang, Z., Zhuo, B., Ti, P., & Yuan, Q. (2021). Effects of different hot pressing processes and NFC/GO/CNT composite proportions on the performance of conductive membranes. *Materials & Design*, 198, 109334.
- [40] Siburian, R., Sihotang, H., Raja, S. L., Supeno, M., & Simanjuntak, C. (2018). New route to synthesise of graphene nano sheets. *Oriental Journal of Chemistry*, 34(1), 182.
- [41] Zeng, Y., Hao, R., Xing, B., Hou, Y., & Xu, Z. (2010). One-pot synthesis of Fe<sub>3</sub>O<sub>4</sub> nanoprisms with controlled electrochemical properties. *Chemical communications*, 46(22), 3920-3922.
- [42] Kestin, J., Sengers, J. V., Kamgar-Parsi, B., & Sengers, J. L. (1984). Thermophysical properties of fluid H<sub>2</sub>O. *Journal of Physical and Chemical Reference Data*, 13(1), 175-183.
- [43] Altun, A., Şara, O. N., & Şimşek, B. (2021). A comprehensive statistical approach for determining the effect of two non-ionic surfactants on thermal conductivity and density of Al<sub>2</sub>O<sub>3</sub>-water-based nanofluids. *Colloids and Surfaces A: Physicochemical and Engineering Aspects*, 626, 127099.
- [44] Altun, A., Şara, O., & Doruk, S. (2022). Sds Surfactant Effects On Stability and Thermophysical Properties Of Al<sub>2</sub>O<sub>3</sub>-Water Based Nanofluids. *Konya Journal of Engineering Sciences*, 10(3), 599-612.
- [45] Selimefendigil, F., Okulu, D., & Oztop, H. F. (2024). Application of ternary nanofluid and rotating cylinders in the cooling system of photovoltaic/thermoelectric generator coupled module and computational cost reduction. *Applied Thermal Engineering*, 250, 123436.
- [46] Sriharan, G., Harikrishnan, S., & Oztop, H. F. (2023). A review on thermophysical properties, preparation, and heat transfer enhancement of conventional and hybrid nanofluids utilized in micro and mini channel heat sink. *Sustainable Energy Technologies and Assessments*, 58, 103327.